

Research Article

A New Microstructure Development Model for the Evaluation of Concrete Setting Time

Ho-Jin Cho,¹ Joo-Won Kang,² Yong Han Ahn,³ Sunkook Kim,⁴ and Xiao-Yong Wang⁵

¹Concrete and Construction Group, DAERIM, Seoul 03152, Republic of Korea

²School of Architecture, Yeungnam University, 280 Daehak-ro, Gyeongsbuk 712-749, Republic of Korea

³Division of Architecture and Architectural Engineering, Hanyang University, ERICA, Ansan-si 15588, Republic of Korea

⁴Multi-Functional Nano/Bio Electronics Lab, Kyunghee University, Gyeonggi 446-701, Republic of Korea

⁵Department of Architectural Engineering, Kangwon National University, Chuncheon-si 200-701, Republic of Korea

Correspondence should be addressed to Yong Han Ahn; yonghan77@gmail.com

Received 28 December 2015; Accepted 21 April 2016

Academic Editor: Yuyin Wang

Copyright © 2016 Ho-Jin Cho et al. This is an open access article distributed under the Creative Commons Attribution License, which permits unrestricted use, distribution, and reproduction in any medium, provided the original work is properly cited.

Concrete is an exceptionally attractive construction material, with stable material supply, adequate fire resistance, and high durability. Its plasticity can be both an advantage and a disadvantage from an engineering point of view, providing versatile shapes via casting and hardening but also requiring a relatively long period of time to reach its design strength. The setting time, or hardening period, needed before the freshly poured concrete can carry a load, which begins once the hydration reaction has commenced, is a key parameter for durability since it directly affects cracking resistance in early-aged concrete. The new analysis technique for calculating setting time that was developed for this study utilizes both percolation theory and the strength development model. To verify the analytical results obtained using the new model, a critical volume ratio of hydrates was determined and a series of final setting times in concrete were experimentally investigated for different temperatures, mineral admixtures (FA: fly ash; GGBFS: ground granulated blast furnace slag), and a chemical admixture (superplasticizer). The results were found to be in good agreement with the model predictions, confirming its potential utility.

1. Introduction

Defects in early-aged concrete due to thermal and autogenous deformation are known to shorten the service life of RC (reinforced concrete) structures. To construct highly durable RC structures, it is thus necessary to take into account the behavior of newly poured concrete during the earliest stages of construction planning. In order to promote the cracking resistance of these structures during construction, the material design, construction methods, and structural design details must all be carefully considered by applying a suitable analytical technique in advance to assess the early age behavior in concrete quantitatively under construction conditions. In a conventional analysis, fresh concrete is assumed to function as a structural element immediately after mixing, but the achievement of reasonable strength actually takes some time after the onset of the hydration reaction and the very early age deformations due to hydration heat and

shrinkage before setting fails to provide any restraint stresses. In order to analyze the behavior of early-aged concrete more precisely, it is therefore necessary to develop an analytical model that adequately represents the setting characteristics of fresh concrete.

The setting characteristics of concrete are largely determined by the hydration process; hence the parameters that govern this process also control the setting behavior of early-aged concrete. Previous research has indicated that the setting behavior of concrete is influenced by its w/b (water to binder) ratio, initial and curing temperature [1, 2], and type and dosage of mineral admixture/chemical admixture [3, 4]. The current study therefore proposes a new analytical model for setting characteristics based on the percolation theory and expanding cluster model that takes into account these influencing factors. A comparison of test and analytical results for final setting time enables the critical volume ratio of hydrates at which freshly poured concrete starts to develop

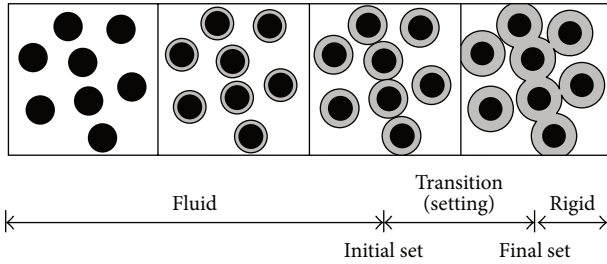


FIGURE 1: Hydration degree and structure formation in fresh cement paste [5].

strength to be determined. We also report the results of an experimental investigation to assess the effect of w/b, curing temperature, mineral admixtures such as fly ash and ground granulated blast furnace slag (GGBFS), and superplasticizer on the setting behavior of early-aged concrete. The information gained in the experimental investigation is discussed and its impact on the setting behavior of the concrete is evaluated and taken into account in the micromodeling of hydration.

2. Definition of Setting Time Based on Percolation Theory

Fresh concrete is a multiphase mixture of cement, water, and aggregates. It transforms from a liquid state to a hardened structure as a result of the chemical reaction involved in the hydration process. The transitional period during which the mixture of fresh concrete changes from a fluid state to a rigid state, shown in Figure 1, is termed the setting period [5].

The process by which concrete sets is divided into an initial and a final setting time. Both the initial and final setting times are arbitrarily defined by the penetration resistance test method, ASTM C 403 [6], which is the most generally used test method. The initial set indicates an approximate time limit for handling and placing the concrete, while the final set represents the onset of the development of mechanical strength [7]. Based on ASTM C 403 [6, 8], the penetration resistances for initial and final setting time are determined to be 3.5 MPa and 27.6 MPa, respectively. The penetration resistance of the final setting time corresponds to 0.7 MPa of the eventual compressive strength for a standard specimen. Recently, a number of innovative techniques for evaluating the setting time have been proposed that utilize ultrasonic, impact-echo, and other specialized sensors [3, 5, 9, 10]. Since the most meaningful setting time in the context of the analysis of early-age concrete behavior is the final setting time, modeling the final setting time is the focus of this study. Figure 2 shows the relationship between rigidity and time for the interval between initial and final setting.

When water and cement are mixed, a process of microstructure development commences, accompanied by nucleation and the growth of hydration products. The hydrates congregate around nucleation centers, in this case the cement particles, to form hydrate clusters. As hydration proceeds, the clusters grow larger and an interconnected solid network begins to develop. Setting starts once the hydrated cement

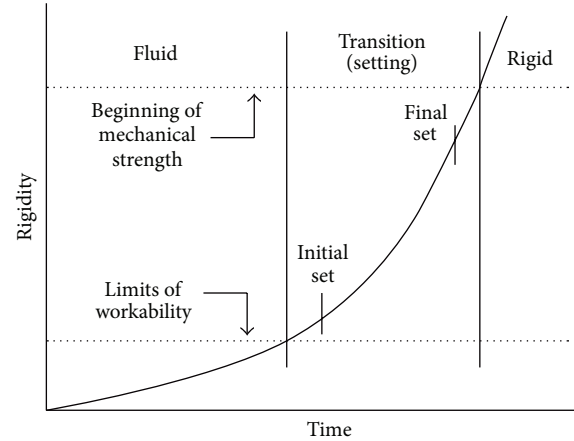


FIGURE 2: Setting time and rigidity based on ASTM C403 [7].

particles begin to be in contact with each other and ends when the cement paste becomes solid. The current consensus among researchers is that setting behavior is best described by the percolation theory, which explains the birth, growth, and linkage of the internal microstructure of hydrating grains [10, 11]. The isolated hydrating grains that are originally spread randomly throughout the volume build up additional layers to form clusters around each grain, which then expand to create connections between them. The fraction of connection that is necessary to allow the transition to a certain action is called the percolation threshold of that action. Garboczi and Bentz [12] investigated the percolation threshold using a digitally based three-dimensional simulation program that simulates the hydration process, concluding that although the degree of hydration at the percolation threshold differs with different w/b (water to binder) ratios, the volume fraction of hydrates remains constant regardless of the mixture conditions. In the current study, the setting time is thus defined based on percolation theory and the volume fraction of the hydrate at the percolation threshold is considered to be invariable.

3. Determination of Critical Volume Ratio Based on the Expanding Cluster Model

3.1. Background of Previous Models: The Expanding Cluster Model

3.1.1. *Stereological Characteristics of Representative Elements of Cement Particles* [13, 14]. Cement particles with various size can be modeled in terms of their stereological characteristics, as shown in Figure 3. In a uniformly dispersed system of spherical particles of radius (r_0), the average volumetric concentration (G) and the mean spacing between the outer surfaces of two particles (s) can be represented by [13]

$$G = \frac{G_0}{(1 + s/2r_0)^3}, \quad (1)$$

where G_0 is the maximum volumetric concentration, whose theoretical maximum is $\pi/3\sqrt{2}$. However, in our proposed

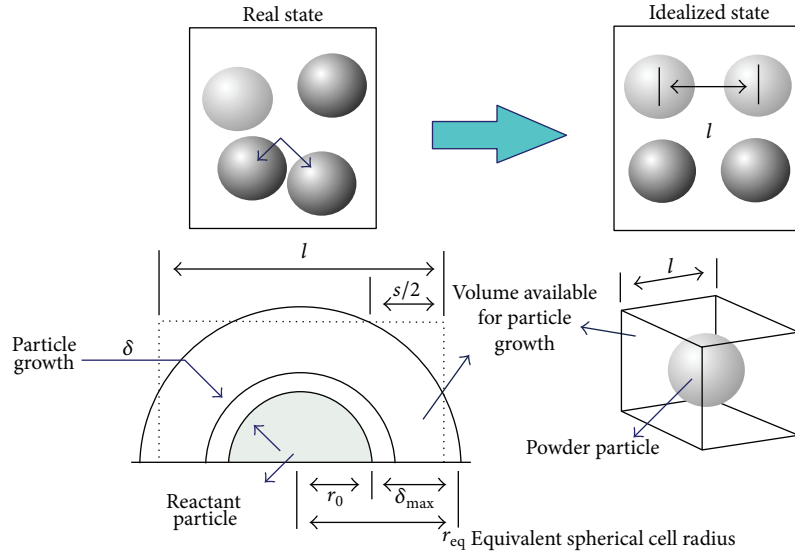


FIGURE 3: Representative unit cell of a powder particle [13].

model G_0 is computed from the following empirical equation, which permits a large spread in the size of particles [13]:

$$G_0 = 0.79 \left(\frac{BF}{350} \right)^{0.1}, \quad G_0 \leq 0.91, \quad (2)$$

where BF represents the Blaine fineness index. If the w/b ratio of particle is ω_0 , the average spacing s between particles can be obtained as follows [13]:

$$s = 2r_0 \left[\left\{ G_0 (1 + \rho_p \omega_0) \right\}^{1/3} - 1 \right], \quad (3)$$

where ρ_p denotes the average specific gravity of the powder.

The initial volume of the cubic cell is transformed into a representative spherical cell of radius (r_{eq}) which can be simply obtained as follows [13]:

$$r_{eq} = \left(\frac{3}{4\pi} \right)^{1/3} l = \chi l, \quad (4)$$

where l is the length of the edge of the cubic cell and χ is the stereological factor. As Figure 3 shows, adjacent particles begin to touch once the thickness of the expanding cluster (δ_m) equals the spacing (s). The equivalent representative spherical cell occurs when the thickness of the expanding cluster equals δ_{max} , as defined in the following expression [13]:

$$\delta_{max} = r_{eq} - r_0 = r_0 \left[2\chi \left\{ G_0 (1 + \rho_p \omega_0) \right\}^{1/3} - 1 \right]. \quad (5)$$

The geometrical parameters, r_0 , r_{eq} , and δ_{max} , are applied to calculate the thickness and volume of the hydrates.

3.1.2. Hydrate Thickness in the Expanding Cluster Model [13, 14]. When hydration commences, an outer product of cement forms on the outer surface and this hydrate thickness increases with time. At the same time, an inner product

develops within the particle due to intruded water. This mechanism of hydration development is known as the expanding cluster model and forms the theoretical basis for the current study. Cluster expansion characteristics are plotted in Figure 4.

The inner product is assumed to have a dense pore structure and constant characteristic porosity regardless of the degree of hydration ($\phi_{in} = \phi_{ch} = 0.28$) [8]. In Figure 4, δ denotes the distance of any point in the cluster from the outer boundary of the particle; δ_m is the thickness of the cluster at the instant of hydration; and ϕ_{ou} and ϕ_{in} are the porosities of the outer and inner products, respectively. In the contact region of the inner product, the porosity becomes ϕ_{in} , and in the outer surface the porosity becomes 1.0. If the thickness of the particle approaches δ_{max} , the porosity in the outer surface gradually decreases with hydration. Utilizing a power function shape, porosity in cluster expansion can be assumed to take the following form [13]:

$$\phi_\delta = (\phi_{ou} - \phi_{in}) \left(\frac{\delta}{\delta_m} \right)^n + \phi_{in}, \quad (6)$$

where n is assumed to be 1.0 for a linear relationship.

To calculate the thickness of the expansion cluster δ_m , a compatibility condition is introduced. The total weight of the product should equal the sum of the inner and outer products, so the total amount of the hydrate product W_T and that of the inner products W_{in} can be obtained from (7) and (8), respectively [13], as follows:

$$W_T = \frac{4}{3} \pi r_0^3 \alpha \rho_p (1 + \beta), \quad (7)$$

$$W_{in} = \frac{4}{3} \pi r_0^3 \alpha \left[\frac{(1 + \beta)(1 - \phi_{in})}{(1/\rho_p + \beta/\rho_u)} \right]. \quad (8)$$

The amount of hydrate material in the outer product W_{ou} can be obtained by integrating the mass present at any arbitrary

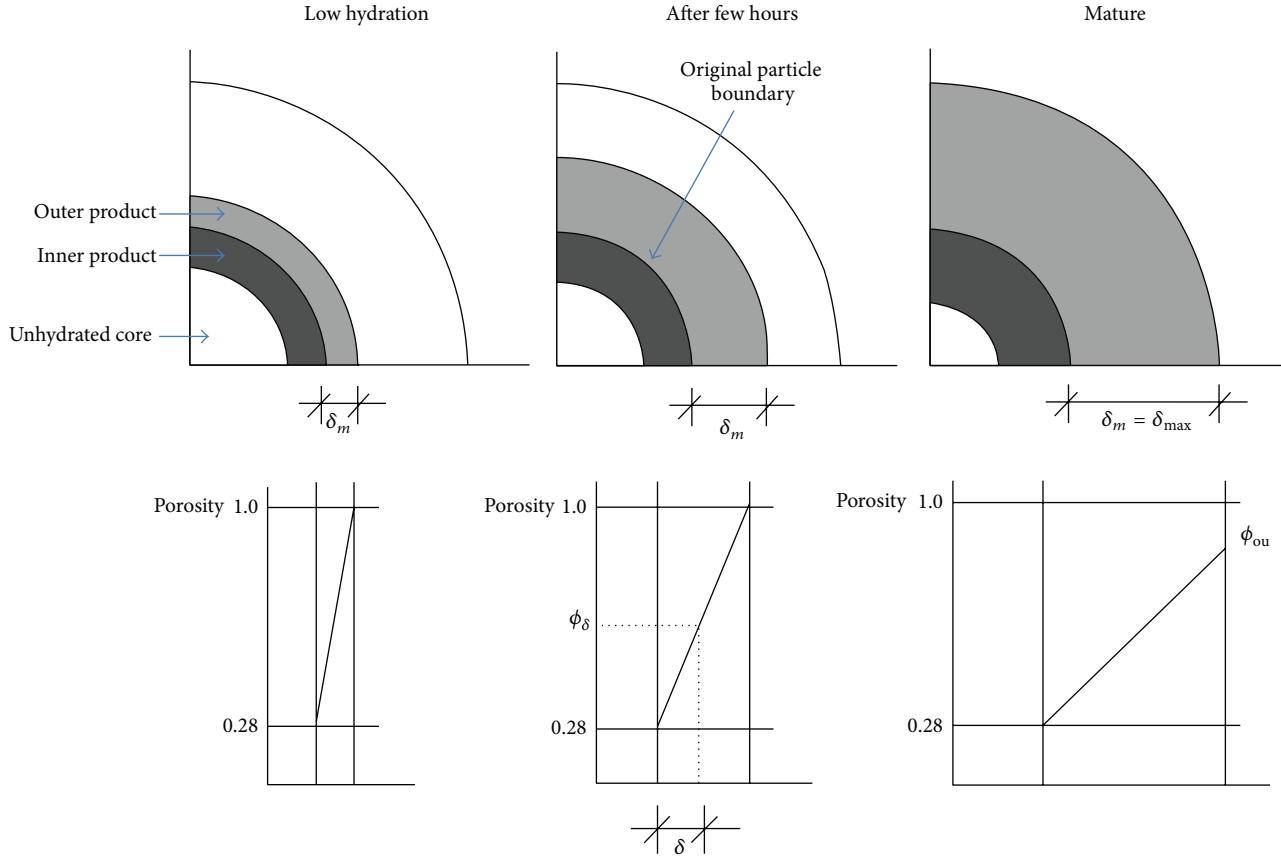


FIGURE 4: Cluster expansion model showing the variation in porosity [13].

location in the cluster over the entire cluster thickness, as follows [13]:

$$\begin{aligned}
 W_{\text{ou}} &= \int_{r_0}^{r_0+\delta_m} 4\pi r^2 \rho_r dr \\
 &= \frac{4\pi(1+\beta)}{1/\rho_p + \beta/\rho_u} \int_0^{\delta_m} [1-\phi_\delta](\delta+r_0)^2 d\delta,
 \end{aligned} \quad (9)$$

where α and β are the hydration degree and the chemically combined water per unit weight of particle, both of which are computed from the multicomponent hydration heat model [13–16]. ρ_p and ρ_u are the density of the powder and pore water, respectively, and ρ_r is the density of the hydrate at a distance r from the surface, obtained as follows [13, 14]:

$$\rho_r = \frac{(1+\beta)(1-\phi_r)}{(1/\rho_p + \beta/\rho_u)}. \quad (10)$$

The compatibility equation ($W_T = W_{\text{in}} + W_{\text{ou}}$) can be combined with (7)–(9) to yield the thickness δ_m . To calculate the variables, the multicomponent hydration heat model [13–16] can be utilized. This model has been adopted and modified for the current application to include a durability analysis for chloride attack [17], water permeation [18], and carbonation in cracked [19] concrete.

3.2. Determination of the Critical Volume Ratio. As mentioned previously, the percolation threshold is defined as the fraction of connection necessary to allow the transition to a certain action to commence. In the case of the final setting time, the percolation threshold is defined as the volume ratio of hydrates that allows load transition. Here, the volume ratio of hydrates at the final setting time is defined as the critical volume ratio. To determine this ratio it is necessary to compare the experimental results for final setting time with the analytical results from the model. The final setting times were measured for three different mix proportions, specified in ASTM C 403 [6] and shown in Table 1. The volume ratio of hydrates at each final setting time, the critical volume ratio, can then be determined by applying a Finite Element (FE) program that combines the aforementioned models [13, 14] to analyze the setting characteristic for fresh concrete. The critical volume ratio is thus proposed as

$$V_r = \frac{(r_0 + \delta)^3 - r_0^3}{(r_0 + \delta_{\text{max}})^3}. \quad (11)$$

OPC (Ordinary Portland Cement) was used as the binder, washed sea sand as the fine aggregate, and crushed stone as the coarse aggregate in this test. The specific gravities of the cement, fine aggregate, and coarse aggregate were measured as 3.15 (g/cm³), 2.58 (g/cm³), and 2.61 (g/cm³), respectively. The test was performed on cement mortar obtained by sieving

TABLE 1: Mix proportions used to determine the critical volume ratio.

w/c ratio	Fine aggregate ratio	Unit content of weight (kg/m ³)			
		Cement	Water	Fine aggregate	Coarse aggregate
0.37	0.38	446	165	665	1,085
0.47	0.42	351	165	767	1,060
0.57	0.45	289	165	845	1,032

TABLE 2: Critical volume ratio and degree of hydration with setting time.

w/c ratio	Test results for final setting time (hours)	Analysis results at final setting time	
		Volume ratio of hydrates	Degree of hydration
0.37	8.12	0.132	0.155
0.47	9.62	0.138	0.184
0.57	10.93	0.139	0.210

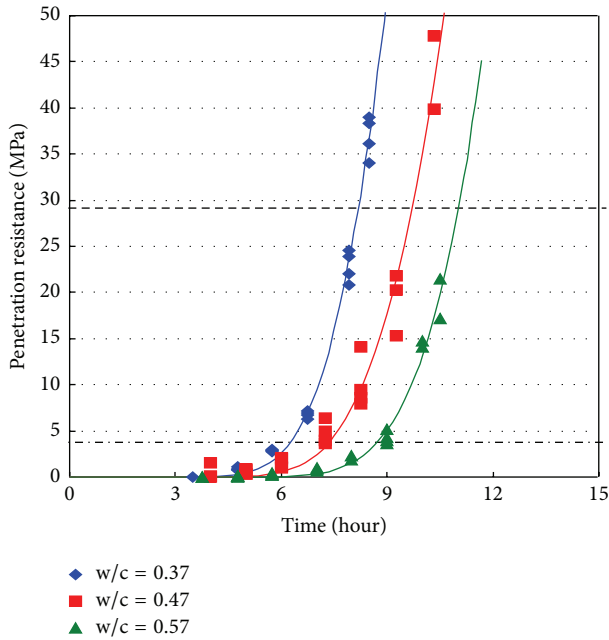


FIGURE 5: Comparison of setting behaviors for different w/c ratios.

freshly mixed concrete through a 5 mm sieve. To minimize the effect of exterior conditions, the specimens were kept in a controlled environment at $20 \pm 1^\circ\text{C}$ during the test. The initial and final setting times were defined as the times at which the penetration resistance reached values of 3.5 MPa and 27.6 MPa, respectively [6, 8]. A graph of the penetration resistance versus time for the three different mixtures is shown in Figure 5. The changes in critical volume ratio and hydration degree obtained from the FE analysis are presented in Table 2 and Figure 6, along with the setting times.

As shown in Table 2 and Figure 6, the volume ratios for the hydrates at the final setting time are in the range 0.13~0.14, while the degrees of hydration fall in the range 0.15~0.21, albeit with relatively large variations. Thus, the critical volume ratio of hydrates can be assumed to be a constant, namely, 0.135. It is clear that this approach, which defines the final

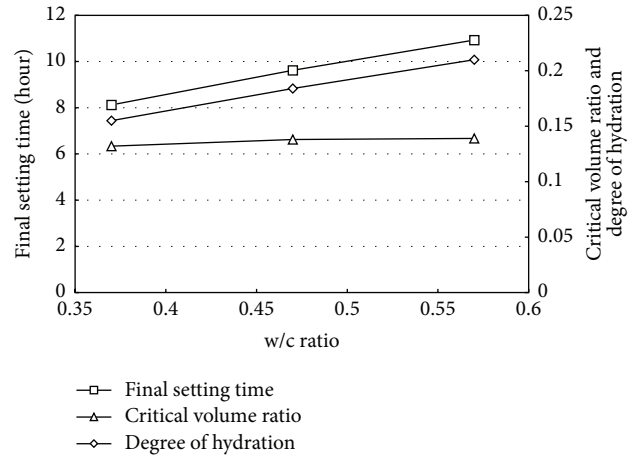


FIGURE 6: Changes in critical volume ratio and hydration degree.

setting time based on percolation theory, is more convenient than approaches based on the degree of hydration.

3.3. Modification of the Previous Model to Account for the Effect of Chemical Admixture. Chemical admixtures such as superplasticizers act as retardation agents, which can delay the time when the calcium rich layer forms by consuming the Ca^{2+} ions created during the initial hydration of the cement. By modifying the models proposed by previous researchers [12, 20], a new parameter, γ , can be introduced to control for the effect of this retardation:

$$\gamma = \frac{v_{\text{total}}\chi_{\text{sp}}}{\text{Ca}_{\text{SUP}}}, \quad (12)$$

where v_{total} is the total amount of organic chemical admixture (% of cement) and χ_{sp} is a parameter that depends on the type of admixture and is an experimentally determined constant. Ca_{SUP} is the admixture's capacity to sequester Ca^{2+} ions; if sufficient Ca^{2+} ion absorption capacity is provided, the retardation effect of the chemical admixture is accomplished more rapidly. Since C_3S is reported to have a greater capacity

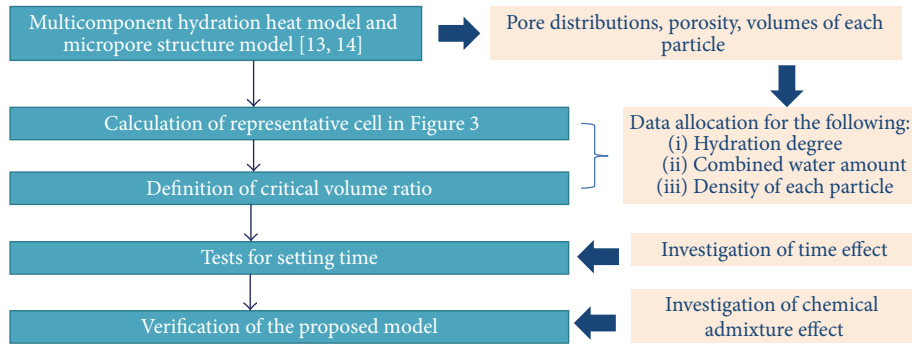


FIGURE 7: Flowchart for test and numerical modeling.

for Ca^{2+} ion supply than C_2S and slag, the following equation is adopted [13]:

$$C_{\text{ASUP}} = \frac{10p_{\text{C}_3\text{S}} + 5p_{\text{C}_2\text{S}} + 2.5p_{\text{SG}}}{1000}, \quad (13)$$

where p_i is the weight percentage of each component (C_3S , C_2S , and slag) and the retardation effect is active only during the initial hydration stage, at levels below 3% of the entire hydration [13, 21].

The flowchart for the entire work is listed in Figure 7.

4. Verification of Setting Behavior Model

4.1. Experiments on Setting Behavior for Various Mixture Conditions. An experimental investigation was also carried out to show the effect of mixture conditions on setting behavior. In order to investigate the effect of curing temperature on setting behavior, two mixtures of different w/c ratios (0.37 and 0.47) cured at 20°C and 40°C were tested; the effect of mineral admixture (fly ash and GGBFS) on setting behavior was also measured. Two different replacement ratios for fly ash (10% and 20% by cement mass) and GGBFS (30% and 50% by cement mass) were tested for a mixture with a w/c ratio of 0.47. Likewise, two different amounts of chemical admixture (superplasticizer) were evaluated (0.375% and 0.75%, as a percentage of cement mass). The Blaine values of the fly ash and GGBFS were $3,630 \text{ cm}^2/\text{g}$ and $4,340 \text{ cm}^2/\text{g}$, respectively. Naphthalene type superplasticizer was used for the chemical admixture. The graphs for the penetration resistance versus time showing the impact of each of these options on the setting behavior of concrete are shown in Figures 8–11.

The effect of curing temperature on the setting behavior is shown in Figure 8. As the curing temperature increases from 20°C to 40°C , the setting time shortens considerably and the time gap between initial and final set is also reduced. As the temperature increased from 20°C to 40°C , the final setting times for the two different w/c ratios decreased by 44.8% (from 8.12 to 4.48 hours) for a w/c ratio of 0.37 and 49.8% (9.62 to 4.97 hours) for a w/c ratio of 0.47, respectively. The observed acceleration in setting times due to the higher curing temperature can be mainly attributed to the temperature dependency of the hydration reaction.

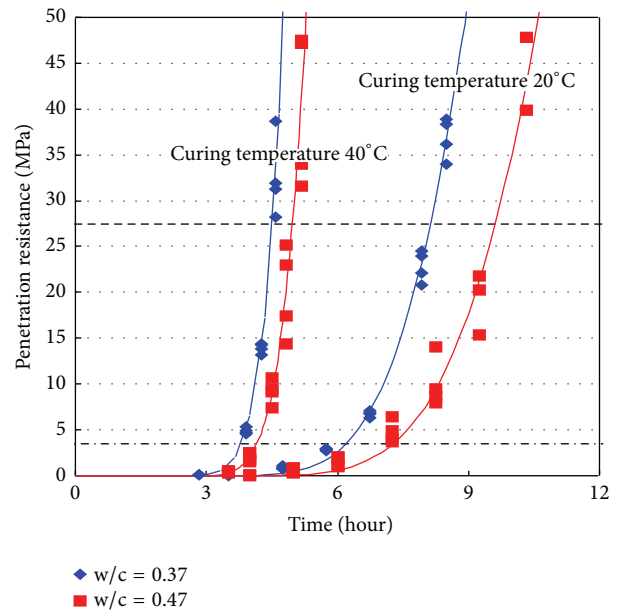


FIGURE 8: Influence of curing temperature on setting behavior of concrete.

Figures 9 and 10 show the influence of the two different mineral admixtures on the setting behavior. As the graphs show, increasing the replacement ratio delays the final setting time; for a 10% fly ash content the setting time is delayed by 6.3% (10.23 hours) increasing to 12.6% (10.83 hours) for a 20% fly ash content. For the case of GGBFS, increasing the content from 30% to 50% lengthens the final setting time from 14.4% (11.0 hours) to 25.8% (12.1 hours). This retardation of the setting time is due to the additive replacing the original relatively inactive mineral admixture. Another reason for the retardation in fly ash concrete is likely the reported release of the SO_3^{2-} present on the surface of the fly ash [8, 22].

The influence of the superplasticizer is shown in Figure 11. Superplasticizers are very effective retardation agents and the resulting delay in the setting time appears to be non-linear with the dosage of superplasticizer, rising from a baseline with no superplasticizer to 19.7% (9.72 hours) and then 34.2% (10.9 hours) with the addition of 0.375% and

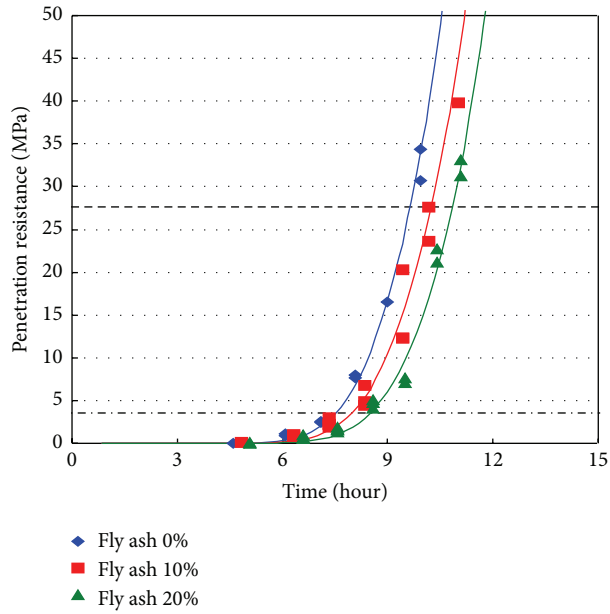


FIGURE 9: Influence of % fly ash content on setting behavior of concrete.

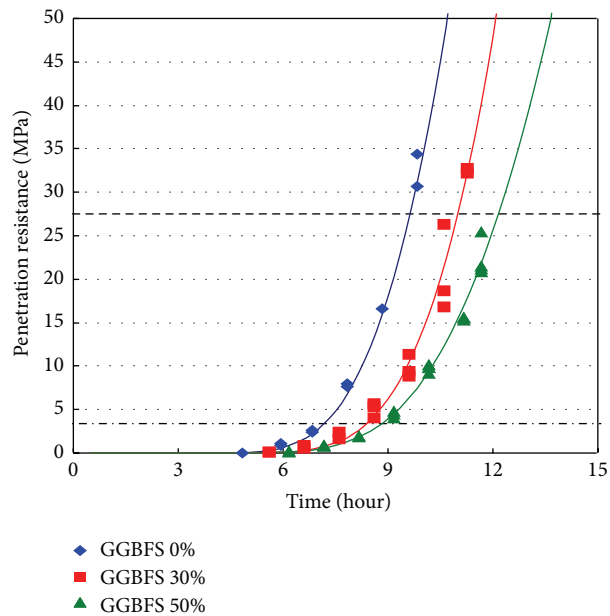


FIGURE 10: Influence of % GGBFS content on setting behavior of concrete.

0.750% of superplasticizer, respectively. The effects of temperature and the various admixtures are summarized in Figure 12.

4.2. *Verification of Analytical Results.* The analytical results obtained using the proposed model, (11) and (12), were verified by comparing them with the experimental results reported above. Table 3 shows that the proposed model achieved a reasonable estimation of the final setting times over the entire range of different mixtures and curing conditions tested, falling within about 4.66% of the experimental

values on average. The results in Table 3 are depicted graphically in Figure 13.

5. Conclusions

In this paper we propose a new analytical model for setting behavior that combines percolation theory with the structure formation model, defining the setting process in fresh concrete in terms of its microstructure development. The proposed model was then verified by comparing its results with those obtained experimentally for a range of different

TABLE 3: Comparison of experimental and analytical results.

Final setting time (hours)	Curing temperature (40°C)		Replacement of admixture (%)					
			Fly ash (w/c 0.47)		GGBFS (w/c 0.47)		Super plasticizer (w/c 0.37)	
	w/c 0.37	w/c 0.47	10%	20%	30%	50%	0.375%	0.75%
Experiment	4.48	4.97	10.23	10.83	11.00	12.10	9.72	10.90
Analysis	4.80	5.28	10.08	11.04	10.56	11.76	9.12	10.08
Error (%)	7.14	6.24	1.47	1.94	4.00	2.81	6.17	7.52

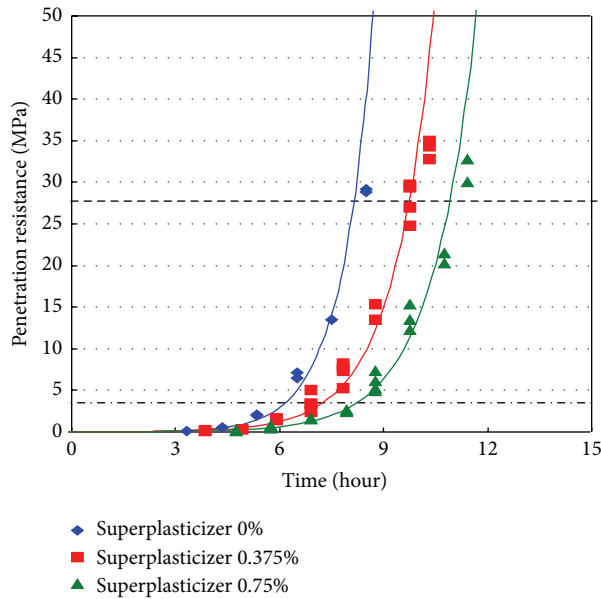


FIGURE 11: Influence of superplasticizer on the setting behavior of concrete.

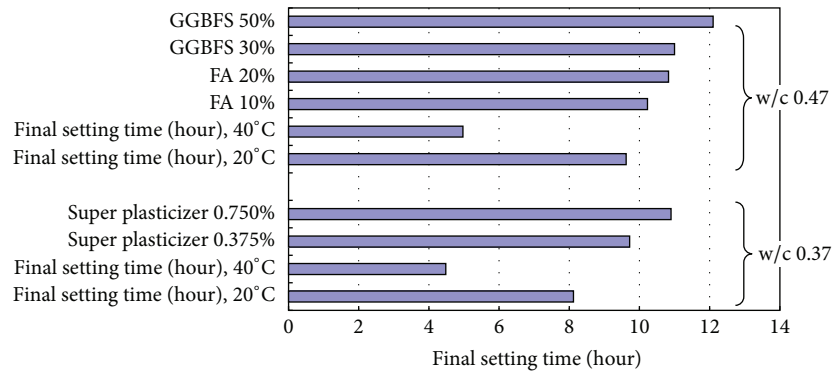


FIGURE 12: Summary of setting times with different temperatures and admixtures.

setting temperatures and admixtures. Our conclusions are as follows:

- (1) A new analytical technique for the evaluation of setting time is proposed that takes into account the critical volume ratio and is based on percolation theory and the cluster expansion model.
- (2) The effects of temperature and mineral admixtures (FA and GGBFS) on setting behavior were investigated experimentally. When the curing temperature increased from 20°C to 40°C, the final setting time

shortened by 55.17% (from 8.12 to 4.48 hours, w/c 37) and 51.67% (9.62 to 4.97 hours, w/c 47), respectively. For mineral admixtures, adding fly ash delayed the final setting time by 6.34% (10.2 hours) at 10% and 12.58% (10.8 hours) at 20%; GGBFS delayed it by 14.35% (11.0 hours) at 30% and 25.78% (12.1 hours) at 50%. The chemical admixture (superplasticizer) was an exceptionally effective retardation agent, delaying the final setting times by 19.7% (9.7 hours) and 34.2% (10.9 hours) with the addition of just 0.375% and 0.750% of superplasticizer, respectively.

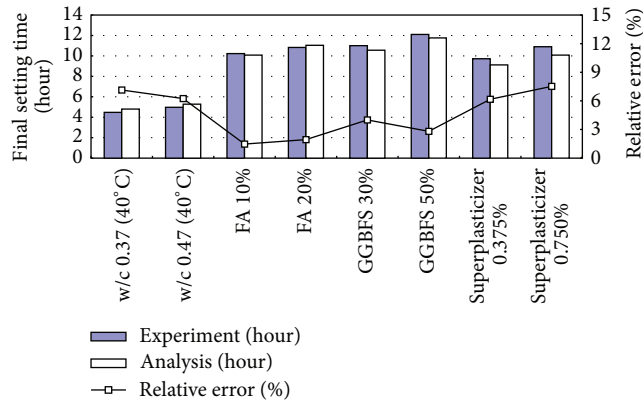


FIGURE 13: Comparison of results and relative error.

- (3) The proposed model for the final setting time developed for this study exhibited a reasonable prediction for concrete with the various admixtures, with the results all falling within a 1.5% ~7.52% relative error range. It is therefore reasonable to conclude that this model offers a potentially useful tool for the evaluation of the setting behavior in early-age concrete.
- (4) The proposed model is only for concrete with FA and GGBFS. For mineral admixtures with high surface area and low density like silica fume, a special parameter which can handle the reduced initial setting time is required. The parameters for chemical admixture are also improved considering Ca^{2+} ion activation of retardation.

Competing Interests

The authors declare that they have no conflict of interests regarding the publication of this paper.

Acknowledgments

This research was supported by the Basic Science Research Program of the National Research Foundation of Korea (NRF) and was funded by the Ministry of Science, ICT & Future Planning (no. 2015RIA5A1037548).

References

- [1] N. I. Fattuhi, "The setting of mortar mixes subjected to different temperatures," *Cement and Concrete Research*, vol. 18, no. 5, pp. 669–673, 1988.
- [2] S. Aggoun, M. Cheikh-Zouaoui, N. Chikh, and R. Duval, "Effect of some admixtures on the setting time and strength evolution of cement pastes at early ages," *Construction and Building Materials*, vol. 22, no. 2, pp. 106–110, 2008.
- [3] S. P. Pessiki and N. J. Carino, "Setting time and strength of concrete using the impact-echo method," *ACI Materials Journal*, vol. 85, no. 5, pp. 389–399, 1988.
- [4] M.-H. Zhang and J. Islam, "Use of nano-silica to reduce setting time and increase early strength of concretes with high volumes of fly ash or slag," *Construction and Building Materials*, vol. 29, no. 4, pp. 573–580, 2012.
- [5] B. Glišić and N. Simon, "Monitoring of concrete at very early age using stiff SOFO sensor," *Cement and Concrete Composites*, vol. 22, no. 2, pp. 115–119, 2000.
- [6] ASTM, "Standard test method for time of setting of concrete mixtures by penetration resistance," ASTM C 403, ASTM Standards, 1999.
- [7] S. Mindess, J. F. Young, and D. Darwin, *Concrete*, Prentice-Hall, Upper Saddle River, NJ, USA, 2003.
- [8] A. M. Neville, *Properties of Concrete*, Addison Wesley Longman, 1995.
- [9] M. I. A. Khokhar, S. Staquet, E. Roziere, and A. Loukili, "Ultrasonic monitoring of setting time of green concrete containing high cement substitution by mineral additions," in *Proceedings of the Non-Destructive Testing in Civil Engineering (NDTCE '09)*, Nantes, France, July 2009.
- [10] V. Garnier, G. Corneloup, J. M. Sprauel, and J. C. Perfumo, "Setting time study of roller compacted concrete by spectral analysis of transmitted ultrasonic signals," *NDT & E International*, vol. 28, no. 1, pp. 15–22, 1995.
- [11] A. Boumiz, C. Vernet, and F. C. Tenoudji, "Mechanical properties of cement pastes and mortars at early ages: evolution with time and degree of hydration," *Advanced Cement Based Materials*, vol. 3, no. 3-4, pp. 94–106, 1996.
- [12] E. J. Garboczi and D. P. Bentz, "The effect of statistical fluctuation, finite size error, and digital resolution on the phase percolation and transport properties of the NIST cement hydration model," *Cement and Concrete Research*, vol. 31, no. 10, pp. 1501–1514, 2001.
- [13] K. Maekawa, R. Chaube, and T. Kishi, *Modeling of Concrete Performance: Hydration, Microstructure Formation and Mass Transport*, Routledge, London, UK, 1999.
- [14] K. Maekawa, T. Ishida, and T. Kishi, *Multi-Scale Modeling of Structural Concrete*, Taylor & Francis, New York, NY, USA, 2009.
- [15] H.-W. Song, H.-J. Cho, S.-S. Park, K. J. Byun, and K. Maekawa, "Early-age cracking resistance evaluation of concrete structures," *Concrete Science and Engineering*, vol. 3, no. 10, pp. 62–72, 2001.
- [16] T. Ishida and K. Maekawa, "Modeling of durability performance of cementitious materials and structures based on thermohydro physics," in *Proceedings of the 2nd International RILEM*

Workshop on Life Prediction and Aging Management of Concrete Structures, vol. 1, pp. 39–49, Paris, France, May 2003.

- [17] S.-S. Park, S.-J. Kwon, and S. H. Jung, “Analysis technique for chloride penetration in cracked concrete using equivalent diffusion and permeation,” *Construction and Building Materials*, vol. 29, no. 4, pp. 183–192, 2012.
- [18] S.-S. Park, S.-J. Kwon, S. H. Jung, and S.-W. Lee, “Modeling of water permeability in early aged concrete with cracks based on micro pore structure,” *Construction and Building Materials*, vol. 27, no. 1, pp. 597–604, 2012.
- [19] H.-W. Song, S.-J. Kwon, K.-J. Byun, and C.-K. Park, “Predicting carbonation in early-aged cracked concrete,” *Cement and Concrete Research*, vol. 36, no. 5, pp. 979–989, 2006.
- [20] T. Kishi and K. Maekawa, “Multi-component model for heat of hydration heating of blended cement with blast furnace slag and fly ash,” *Concrete Library of JSCE*, vol. 30, no. 12, pp. 125–139, 1997.
- [21] H.-J. Cho, H.-W. Song, and K. J. Byun, “Development analytical model on setting characteristics of early-age concrete,” *Journal of Korea Society Civil Engineering*, vol. 23, no. 3, pp. 549–557, 2003.
- [22] S. W. Yoo, S.-J. Kwon, and S. H. Jung, “Analysis technique for autogenous shrinkage in high performance concrete with mineral and chemical admixtures,” *Construction and Building Materials*, vol. 34, no. 9, pp. 1–10, 2012.



Hindawi

Submit your manuscripts at
<http://www.hindawi.com>

